HAL
open science

Conducted EMI of Integrated Switching Audio Amplifier for Mobile Phone Applications

Salah-Eddine Adami, Roberto Mrad, Florent Morel, Christian Vollaire, Gaël Pillonnet, Rémy Cellier

To cite this version:

Salah-Eddine Adami, Roberto Mrad, Florent Morel, Christian Vollaire, Gaël Pillonnet, et al.. Conducted EMI of Integrated Switching Audio Amplifier for Mobile Phone Applications. EMC Compo, Nov 2011, Dubrovnik, Croatia. pp.142-147. hal-00641582

HAL Id: hal-00641582

https://hal.science/hal-00641582v1

Submitted on 16 Mar 2015

HAL is a multi-disciplinary open access archive for the deposit and dissemination of scientific research documents, whether they are published or not. The documents may come from teaching and research institutions in France or abroad, or from public or private research centers.

L'archive ouverte pluridisciplinaire **HAL**, est destinée au dépôt et à la diffusion de documents scientifiques de niveau recherche, publiés ou non, émanant des établissements d'enseignement et de recherche français ou étrangers, des laboratoires publics ou privés.

Conducted EMI of Integrated Switching Audio Amplifier for Mobile Phone Applications

S-E. Adami, R. Mrad, F. Morel, C. Vollaire
AMPERE Laboratory
University of Lyon, Ecole Centrale de Lyon
Lyon, France
Salah-eddine.adami@ec-lyon.fr

G. Pillonnet, R. Cellier
Lyon Institute of Nanotechnology
University of Lyon, CPE Lyon
Lyon, France
inl@cpe.fr

***Abstract*—In this paper, conducted EMI measurements of two integrated Class D audio amplifiers are realized using the EN55022 standard, in order to compare the EMI behavior of two modulation techniques. The first circuit uses a carrier-based pulse-width modulation (PWM) and the second uses a self-oscillating modulation based on sliding-mode (SM) control. Measurement results show that SM circuit has better EMI behavior compared to PWM circuit, thanks to spread spectrum effect of the SM circuit. Spice simulations using full transistor circuit model are realized to evaluate the range of validity of the used model in large frequencies. Simulation results are very closed to the measurement ones, especially for low and medium frequencies (up to 10 MHz).**

Keywords- Switching Mode Audio Amplifier, Class D, Low EMI, EMC measurement.

I. INTRODUCTION

Nowadays, embedded system (ES) autonomy is increasingly problematic: with the integration of more and more features, with the increase of processors' frequencies, the autonomy of batteries is more and more threatened. Thus, ES manufacturers look for more energy-efficient circuit designs, such as switching converters. Among these switching converters, there are SMPS (Switching Mode Power Supplies) and Class D dedicated respectively to power supply management and audio amplification. The Class D audio amplifier is attractive due to its high efficiency (100% in theory). Recent research work has developed efficient closed-loop control structures in order to correct the amplification errors introduced by the power stage [1-2]. Thus, using a well-designed feedback structure, Class D can reach high audio performances, i.e. comparable to that of linear audio amplifier performances (e.g. Class AB) [3]. However, manufacturers are suspicious towards EMI (ElectroMagnetic Interference) problems which they risk having when integrating high power high frequency (HF) switching circuits into theirs platforms. Indeed, Class D amplifiers, also called audio switching amplifier, switch relative high current (~1A) with fast rise and fall times (~few ns) at high switching frequencies (from a few hundreds of kHz to some MHz). These transitions generate high-frequency disturbances which propagate outside the Class D circuit (especially through connections between amplifier and speaker and between the amplifier and the battery) and then can disturb neighboring circuits. Knowledge of high frequency switching disturbances is therfore fundamental for the design of quiet class D amplifier. This gives in particular precious data for EMI filter design. In general, Spice simulation based on the semiconductor design kit provides precise results in audio band and for the first few switching harmonics [4]. However, for higher frequencies, the modeling of HF disturbance components (internal silicon rails, bonding, leads, PCB, edges, manufacturing defects...) is very delicate to include in the modeling, which gives a high frequency spectrum that is not realistic. For this reason, manufacturers prefer using some design rules [5] based on their previous experiments to deal with EMI problems: spread spectrum modulation [6], components placement optimization, trace routing reduction, power decoupling, grounding placement, etc. These techniques are as useful in order to reduce EMI, but are not always sufficient to avoid all undesired disturbances. In this case, the system engineer spends much time trying to resolve the problem by several experiments on the final board. Thus, high integrated embedded systems, such as mobile phones, require a thorough knowledge of the phenomenon, i.e. knowledge how, where and why class D audio amplifier emits, also, knowledge of the influence of each part of the circuit on the emission spectrum. All this information can be obtained only by a rigorous measurement procedure associated with a root cause analysis.

The objective of this paper is to define a measurement procedure to characterize the conducted EMI from an integrated Class D amplifier. Then, these practical measurements are compared to Spice simulations to evaluate the model limits. Two Class D with different switching modulation techniques are under these tests: one fixed frequency Pulse Width Modulation (PWM) and one Self Oscillating (SO) modulation.

A brief overview of Class D audio amplifier is provided in Section II.A. In Section II.B, the EMI sources from Class D are identified and in Section II.C a description of the class D under test is given. The Section III focuses on modulation techniques comparison: first, theoretical comparison is made, then conducted EMI measurements are presented. Spice simulations are realized in section III.C and are compared with the experimental measurements. Finally, a conclusion is given in section IV.

II. CLASS D AUDIO AMPLIFIER

A. *Class D amplifier operating principle*

The basic Class D topology and the signal spectrum of each stage are shown on Fig. 1. The spectrum is composed by a modulation stage which transforms a low frequency analog audio input signal to a high frequency modulated bit stream V_{mod}. Then, a power stage translates the bit stream to power supply rails V_{out} in order to feed the load. A low pass filter reduces the high frequency components to restore the original audio signal V_{in} into the speaker. There are various modulation techniques in Class D amplifier which can be classified in two different categories: the fixed frequency modulation schemes (sigma delta modulation, PWM) and the self-oscillating modulations (spread spectrum PWM, hysteresis).

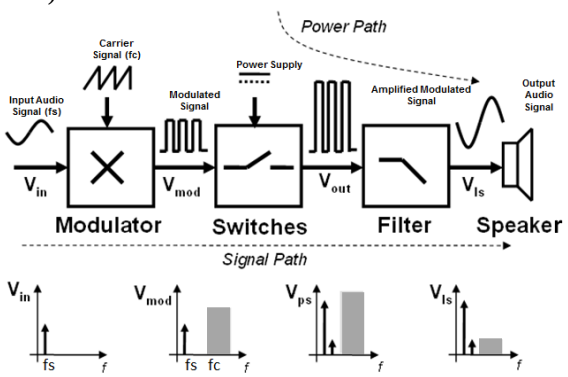

Figure 1. Class D audio amplifier basic bloc diagram

B. *Switching power stage: the main EMI source*

The power stage is composed of two large integrated power MOS transistors (PMOS and NMOS) as shown in Fig. 2. The switching power stage is the principal EMI source. The power stage draws a pulsed current from the power supply. These current spikes coupled with the parasitic elements present between the integrated circuit (IC) and the power source (bonding, lead, PCB) generates high frequency variations in the power supply voltage.

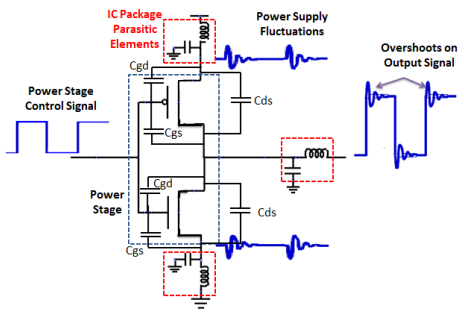

Figure 2. EMI phenomena on the switching power stage

At the output ports, there is another problem: the pulsed signal already contains high frequency harmonics that can cause EMI problems when the signal is propagated to the connection between circuit and speaker.

C. *Class D amplifiers under test*

1) *Topology*

To evaluate and compare the effect of two different modulation techniques, two Class D amplifiers are used in the same configuration: the same output (H-bridge connection to the load, three levels modulation), the same switching power stage, the same packaging and PCB. They differ by their closed-loop modulation control blocs. The first circuit uses a fixed frequency PWM modulation and the second circuit use self-oscillating by using sliding mode control (SM) [7]. Both idle switching frequencies are fixed at 512 kHz. These Class D amplifiers provide about 1W into an 8Ω load, under 3.6V power supply. The audio linearity is higher than 0.1% at 1kHz, and the Signal to Noise Ratio (SNR) is 96dB.

2) *Integrated design*

The integrated analog design of both Class D amplifiers was done using CMOS 0.13µm technology. The electrical schematic and layout for a fixed frequency PWM Class D are shown on Fig. 3 and Fig. 4, respectively. The chip is composed by two operational amplifiers with their networks (C, Rin, Rfb), two comparators, two buffers, two switching power stages and differential output. The filter associated with the load is connected in H-bridge. The output filter (Lext, Cext) are not integrated on the chip. Rl represents the equivalent speaker resistance.

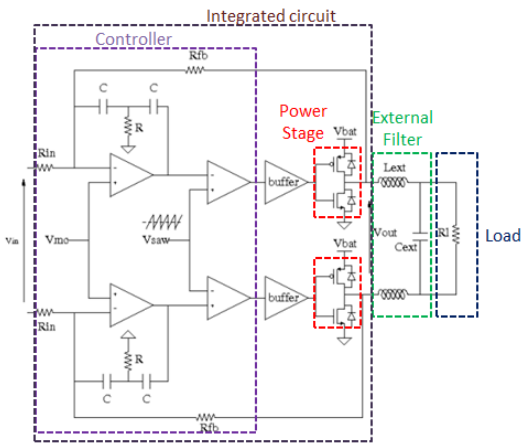

Figure 3. Electrical schematic of fully-integrated Class D amplifier

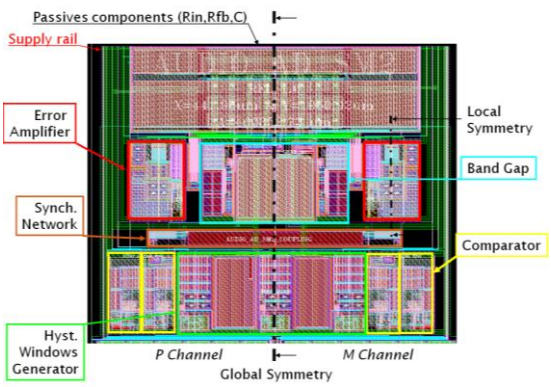

Figure 4. Class D amplifier layout

3) Environment and application

Thin Quad Flat Package (TQFP) is used in both circuits. The same PCB has been designed for the two circuits in order to fit with the IC package. A decoupling capacitor has been chosen to reduce the noise disturbance, as used in a typical mobile phone platform. A shielded inductor and a capacitor make up the external filter.

III. MODULATION TECHNIQUES COMPARISON

A. PWM and SM modulation spectra

1) Pulse width modulation

Carrier based PWM is the widely-used modulation method due to its fixed switching frequency and to design rules maturity. Pulsed signal is generated by comparing audio signal with a sawtooth signal (from a few hundred of kHz to some MHz). A differential circuit structure is used to reduce the effect of noise perturbations and this leads to a ternary modulated signal (Fig. 5).

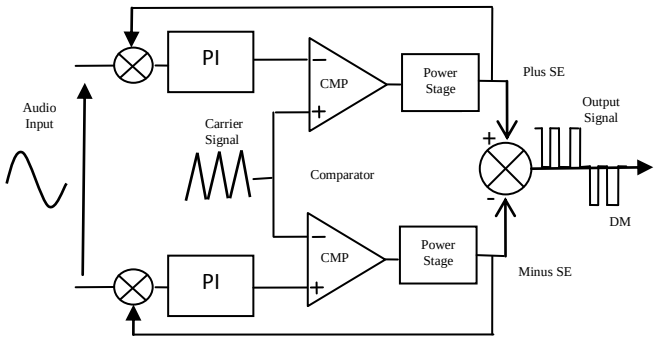

Figure 5. Ternary PWM block diagram

In classical differential modulation, i.e. binary modulation, there are only two possible states: V+ and V-. However, in ternary modulation, there are three possible states: V+, V- and 0 (Fig. 6). This gives a smaller differential signal on the load when a zero audio signal is applied, which leads to an optimization of the idle consumption and also reduces EMI.

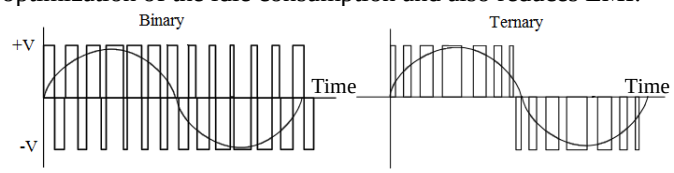

Figure 6. Comparison of ternary and binary modulations

2) Sliding mode modulation

The hysteresis feedback controller generates variable frequency switching signals on each side of the load (plus SE and minus SE). As these two signals have different phases, a synchronization block is added in order de synchronize the two sides of the amplifier (Fig. 7).

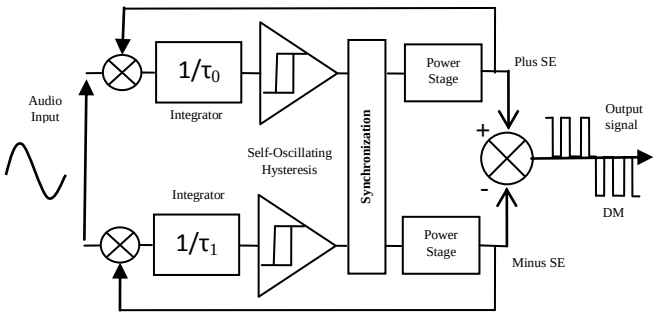

Figure 7. Sliding mode block diagram

The hysteresis stage has an inherent behavior which is to vary its switching frequency, this phenomenon leads to a spreading of the switching frequency. In other words, the switching frequency depends on the modulation index (and on other parameters), i.e. if the audio signal level is very low, then, there is no spread spectrum, and if it is high, the spread spectrum effect is maximal.

3) Theoretical spectra

Theoretical spectra of the power stage signals are presented in Fig. 8. The SM spectrum is spread around the switching frequency (fsw) and its harmonics. This very interesting property allows a significant lowering of the maximal HF spectrum level, leading to a reduction of EMI.

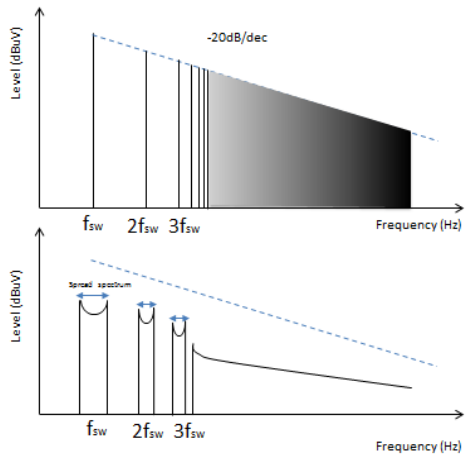

Figure 8. Theoretical spectra: PWM (top) and SM (bottom)

B. Conducted measurements

Class D audio amplifier could cause EMI problems for their environment via two ports: power supply and output ports.

1) Measurement bench presentation

The EN55022 standard [8] for information technology equipment has been used to perform these conducted measurements. This standard recommends the use of a Line Impedance Stabilized Network (LISN). Fig. 9 shows the internal topology for a 50µH LISN. It has one input port for the main power supply and two output ports: the first port is used to feed the Equipment Under Test (EUT) and the second

port is a 50Ω RF output port to connect a broadband spectrum analyzer (EMC Receiver). All the perturbations generated by the EUT are redirected to this port.

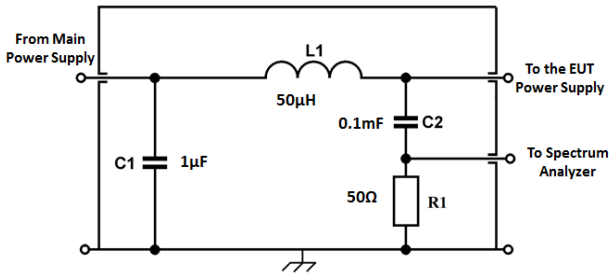

Figure 9. 50µH LISN used in standardized power supply EMI measurements

Fig. 10 shows the used test-board. The integrated circuit (test-chip) contains two class D audio amplifiers (right and left) for stereo mode. The same Test-board and same package are used for both class D test-chips (i.e. PWM and SM).

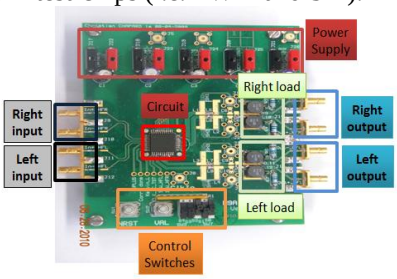

Figure 10. Test-board

Audio amplifiers are connected to an (8Ω + 2x25µH) load which emulates a speaker. On the test-board, there are multiple power supply ports in order to isolate each circuit from another (power stage, control, board control). In order to avoid HF noise from the power supply, battery-powered low-noise linear regulators have been used to feed the different circuits.

The measurement bench is shown in Fig. 11. The spectrum analyzer is connected to the RF output of one of the two LISN. The other LISN RF output is connected to an adapted load of 50Ω.

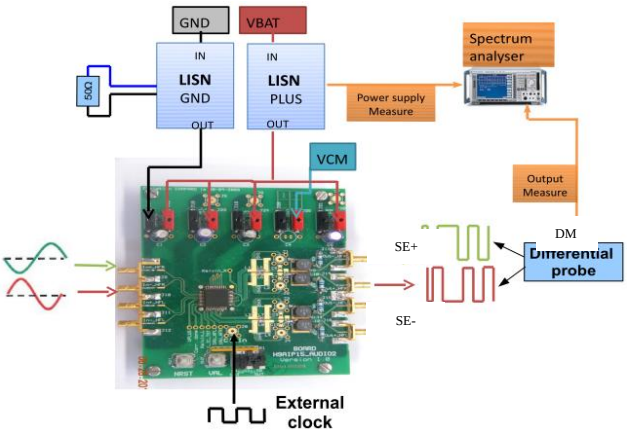

Figure 11. Simplified diagram of the measurement bench

For output measurements, a broadband differential voltage probe is connected to the spectrum analyzer. Each simple output is called Single-Ended (SE). The differential output is called Differential Mode (DM). The input audio signals are two 1kHz differential sinus signals with 0.25Vrms of amplitude. As Class D has 6dB voltage gain, this leads to a 1Vrms at the output (Full scale). Tab. 1 presents used device references.

Device	*manufacturer*	*Reference*	*Bandwidth*
Spectrum analyzer	Rohde & Schwarz	ESPI	9k-7GHz
Acquisition Software	Rohde & Schwarz	EMC32	-
LISN	-	EN55022	150k-30MHz
Differential voltage probe	Agilent	1142A	< 200MHz

TABLE I. USED DEVICES REFERENCES

The frequency range for power supply measurements is 150k-30MHz as advocated by the EN55022 standard, while the range is 18kHz-100MHz for output measurements.

2) Power supply measurements results

Fig. 12 shows measurement results for PWM and SM circuits. The current drawn from the power supply corresponds to a differential operation of the circuit, thus, the highest amplitude frequency is equal to 1024 kHz, i.e. twice the power stage switching frequency. The 512kHz spike comes from the controller current consumption.

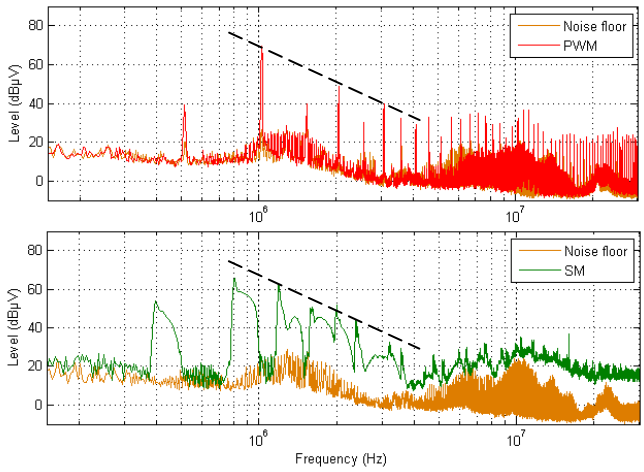

Figure 12. Power Supply measures: PWM circuit (top) and SM circuit (bottom)

The spread spectrum effect on SM spectrum reduces the EMI at around twice the switching frequency (2fsw). At the highest frequency (more than 10 times fsw), the conducted EMI strongly depends on parasitic elements which differ for the two ICs (variation in packaging and production process), despite the fact that both IC circuits have the same packages and same PCB.

3) Output measurements results

The spectrum in Fig. 13 corresponds to Single Ended (SE) output. The SM is decidedly better than PWM especially from 3MHz (at least 6dB lower at arround 50 MHz).

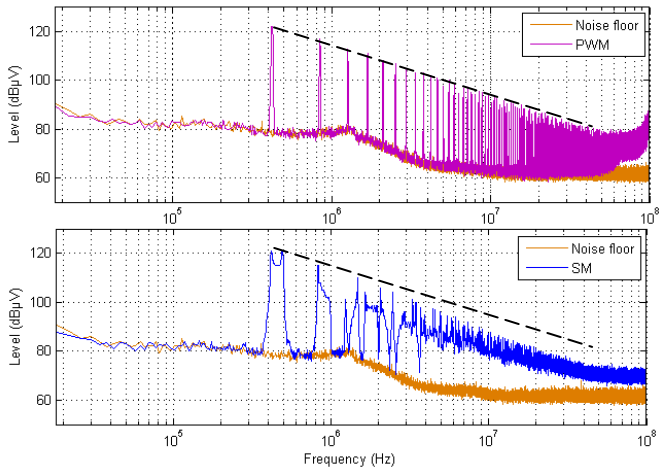

Figure 13. Output measurements for Single Ended (SE): PWM (top) and SM (bottom)

The differential output measurements are presented in Fig. 14. A DM spectrum normally contains only the even harmonics, whereas in these spectra, the odd harmonics presents are due to an imperfect differential input audio signal and mismatch on both differential channels.

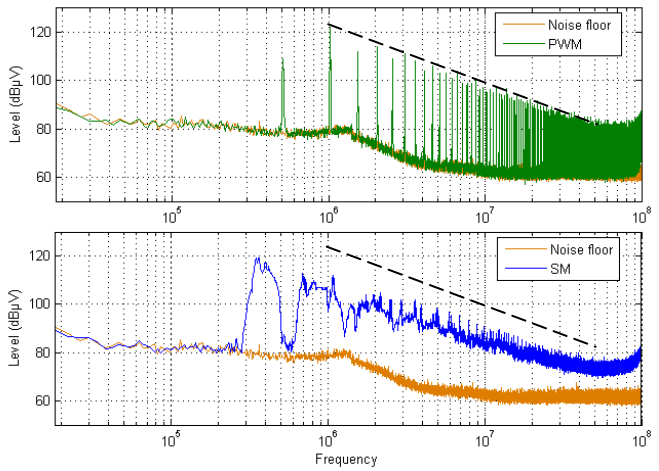

Figure 14. Output measurements for Differential Mode (DM): PWM (top) and SM (bottom)

SM modulation has a lower high frequency spectrum, thanks to the spread spectrum effect. For SE and DM spectra, there is a resonance near 100 MHz; this is certainly due to the output signal overshoots.

C. *Towards EMI prediction by simulation*

Spice simulations using the 0.13µm design-kit (BSIM3v3 level) have been realized. Power supply simulations are not presented here for two reasons: on the one hand, modeling all parasitic elements for power supply is very delicate because all power supplies are coupled via the same ground plane. On the other hand, Spice simulations of the LISN present convergence problems [9], yet unsolved. therefore, only output measurements are presented here.

The simulation block diagram is presented Fig. 15. As there are multiple power supply and ground ports, one pad model block is used for each port. An Anti-Aliasing filter (AAF) is used in order to avoid aliasing problems when output signals are sampled in order to perform Fast Fourier Transform (FFT) computation. The temporal windows contain one period of the 1kHz audio signal. In order to obtain a spectrum up to 100MHz, a sampling frequency Fs = 226MHz is chosen. The anti-aliasing filter has 63dB attenuation at Fs/2 (Nyquist frequency).

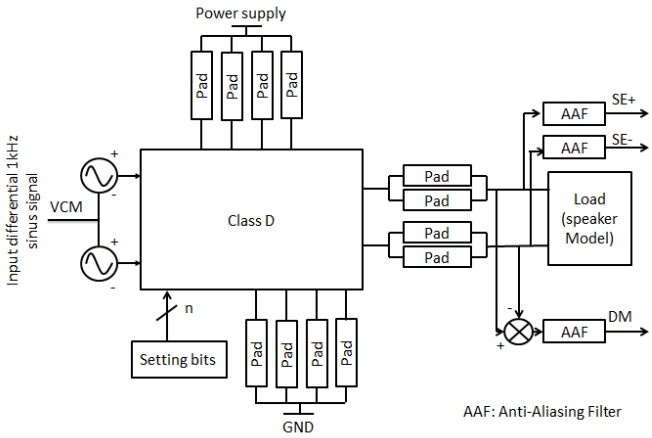

Figure 15. Simulation block diagram

Loud-speaker and pad models are given in Fig. 16 and Fig. 17. The pad model was obtained from experimental measurements. Theoretical calculations show that this model has a resonance frequency around 270MHz. This result cannot be verified experimentally since simulations are performed up to 100MHz. However, it gives an idea of the frequency band over which the integrated circuit package acts.

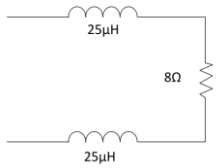

Figure 16. Speaker model

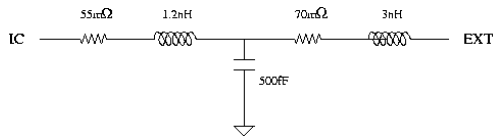

Figure 17. Package (bonding + lead) model for each pin (Pad).

Simulation results fit measurement results and especially for low and medium frequencies (Fig. 18 and Fig. 19). The used model shows its limits from 10MHz. As discussed previously, odd harmonics present in the measured spectrum are due to an imperfect symmetrical input audio signal, and also due to matching problem of the two channels.

The noise floor is higher for measurements than for simulation because of measurement equipment noise. This noise floor is around 80dBµV (i.e. 10mV) which is totally acceptable.

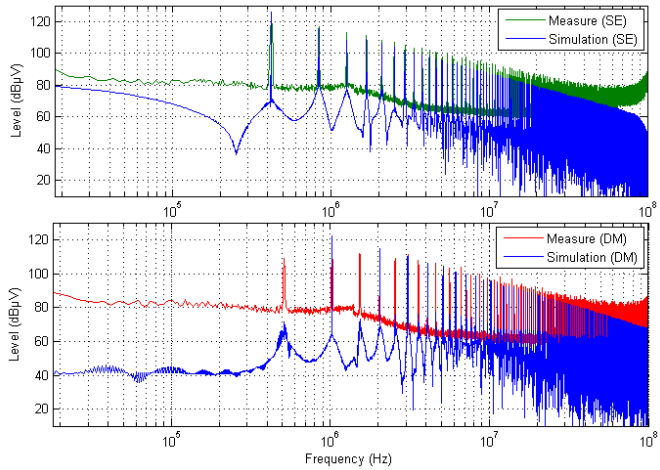

Figure 18. Simulation versus Measurements for the PWM circuit: SE (top) and DM (bottom)

For the SM circuit, there is an excellent similarity between simulation and measurement results for SE.

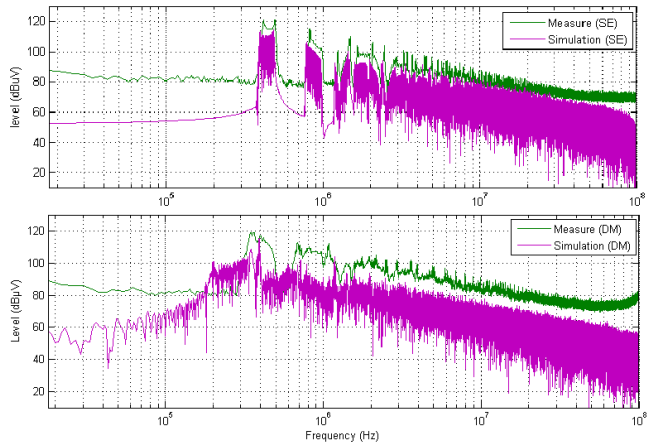

Figure 19. Simulation versus measurements for the SM circuit: SE (top) and DM (bottom)

At higher frequencies (near 100 MHz) the limitations of the used model appear. In fact, only the integrated circuit package model has been considered. Disturbances near 100 MHz certainly come from PCB tracks and unmolded high frequency transistor behavior. The next step consists in PCB tracks modeling in order to make a precise prediction for higher frequencies.

IV. Conclusion

A measurement bench conform to the EN55022 EMC standard has been realized. This allows rigorous and repeatable measurement of high frequency noise generated by Class D circuits. Measurement results show that Sliding Mode (SM) circuit has a lower high frequency spectrum compared to PWM circuit, thanks to spread spectrum effect of the SM modulation. Simulation reveals the model limits for high frequencies (up to 10 MHz). The impedance matrix method [10] will be used in the future to model PCB tracks, in order to obtain better accuracy even for higher frequencies (up to 100 MHz).

Although the spread spectrum technique is very effective in reducing the EM spectrum for low and medium frequencies, it does not have an impact on RF bands, i.e. near 1GHz [11]. Instead, at these frequencies, the spread spectrum disperses spectrum and make it more difficult to filter. For such very high frequencies other EMI reduction techniques have to be used [12]. The choice of a modulation technique then depends on the application on which the switching amplifier will be used.

References

[1] Wei Shu, Chang, J.S., Tong Ge, Meng Tong Tan, "Fourier Series Analysis for Nonlinearities Due to the Power Supply Noise in Open-Loop Class D Amplifiers," Circuits and Systems, 2006. APCCAS 2006. IEEE Asia Pacific Conference, pp.720-723, 4-7 Dec. 2006.

[2] A. Pietro; N. Flemming; R. Lars, “Time Domain Analysis of Open Loop Distortion in Class D Amplifier Output Stages”, 27 International AES Conference, sept. 2005.

[3] Pillonnet, G.; Abouchi, N.; Cellier, R.; Nagari, A.; , "A 0.01%THD, 70dB PSRR Single Ended Class D using variable hysteresis control for headphone amplifiers," Circuits and Systems, 2009. ISCAS 2009. IEEE International Symposium on, pp.1181-1184, 24-27 May 2009.

[4] Gonzalez, D.; Gago, J.; Balcells, J.; , "New simplified method for the simulation of conducted EMI generated by switched power converters," Industrial Electronics, IEEE Transactions on , vol.50, no.6, pp. 1078-1084, Dec. 2003.

[5] Tarui, Y.; Watanabe, K.; Sakusabe, T.; Takahashi, T.; Schibuya, N.; , "EMC constraint PCB design support tool-assistance for power and ground trace wiring," Electromagnetic Compatibility, 1999 International Symposium on, pp.564-567, 1999.

[6] Santolaria, A.; Balcells, J.; Gonzalez, D.; Gago, J.; Gil, S.D.; , "EMI reduction in switched power converters by means of spread spectrum modulation techniques," Power Electronics Specialists Conference, 2004. PESC 04. 2004 IEEE 35th Annual , vol.1, pp. 292- 296 Vol.1, 20-25 June 2004.

[7] Pillonnet, G.; Cellier, R.; Abouchi, N.; Chiollaz, M.; , "An integrated class D audio amplifier based on sliding mode control," Integrated Circuit Design and Technology and Tutorial, 2008. ICICDT 2008. IEEE International Conference on, pp.117-120, 2-4 June 2008.

[8] CISPR 22, Information Technology Equipment—Radio Disturbance Characteristics—Limits and Methods of Measurement, 1997.

[9] Crebier, J.C.; Roudet, J.; Schanen, J.L. "Problems using LISN in EMI characterization of power electronic converters," Power Electronics Specialists Conference, 1999. PESC 99. 30th Annual IEEE , vol.1, pp.307-312 vol.1, Aug 1999.

[10] R. Mrad, F. Morel, C. Vollaire, G. Pillonnet, D. Labrousse. "Passive Circuit Modelling with Pentapole Impedance Matrices" EMC Europe Conference, 2011, in press.

[11] Balcells, J.; Santolaria, A.; Orlandi, A.; Gonzalez, D.; Gago, J.; , "EMI reduction in switched power converters using frequency Modulation techniques," Electromagnetic Compatibility, IEEE Transactions on , vol.47, no.3, pp. 569- 576, Aug. 2005.

[12] Ogasawara, S.; Igarashi, T.; Funato, H.; Hara, M.; , "Optimization of switching transient waveform to reduce EMI noise in a selective frequency band," Energy Conversion Congress and Exposition, 2009. ECCE 2009. IEEE, pp.1679-1684, 20-24 Sept. 2009.